

Comparative study of enhanced fluorescence from nano sculptured thin films

I. Abdulhalim,^{a)} Alina Karabchevsky,^{a)} Christian Patzig,^{b)} Bernd Rauschenbach,^{b)} Bodo Fuhrmann^{c)}

^{a)} Department of Electrooptic Engineering
Ben Gurion University of the Negev, Beer Sheva 84105, Israel

^{b)} Leibniz-Institut für Oberflächenmodifizierung e.V., Permoserstrasse 15, 04318 Leipzig, Germany

^{c)} Interdisziplinäres Zentrum für Materialwissenschaften, Martin-Luther-Universität Halle, Heinrich-Damerow-Straße 4, 06120 Halle

ABSTRACT

When an electromagnetic wave interacts with a nano structured metallic surface or a nanoparticle, the electromagnetic fields near the surface are greatly enhanced by factors up to 1000. This phenomenon is due to two processes: (i) the ‘lightning rod’ effect, conventionally described as the crowding of the electric field lines at a sharp metallic tip and (ii) the excitation of localized surface plasmons at the metal surface. Both are responsible for the enhancement of fluorescence, second-harmonic generation and Raman scattering. For metal nanoparticles often both processes are involved in creating the localized enhanced near field. Since sculptured thin films (STFs) can have a rod like structure and an overall large porosity, it is expected that these structures will exhibit enhanced fluorescence and Raman signals. Results of comparative study of surface enhanced fluorescence are presented from STFs containing metal nano structures. The highest enhancement is found for Ag based STFs giving an enhancement factor of x14.

1. INTRODUCTION

Metal based nano-structures are becoming more and more practically important for photonic devices, particularly for sensing applications, due to the surface enhanced phenomena they exhibit. A number of physicochemical effects related to the behavior of fluorophores near nanoparticles have been brought into focus by this emerging field of plasmonics. Among these, surface enhanced fluorescence (SEF) is one of most useful phenomena^{1,2,3,4,5,6,7,8}, with significant applications in biotechnology and life sciences, alongside with the surface enhanced Raman scattering (SERS). When a molecule is excited, there are a variety of processes which will return it to ground state. If we consider three processes for returning to the ground state (radiationless energy loss, intersystem crossing through the triplet state, and emission of photons) then the efficiency of emission will be a function of the competing rates of these processes:

$$\eta = \frac{K_f}{K_f + K_i + K_x} \quad (1)$$

Where η is efficiency or quantum yield which is a dimensionless quantity given by the ratio between the emitted photon and the number of absorbed photons. The rate constants $K_{f,i,x}$ designate those for fluorescence emission, radiationless energy loss, and intersystem crossing, respectively. The average lifetime of the excited state is inversely related to the fluorescence emission rate: $\tau_f = K_f^{-1}$.

Surface enhanced fluorescence (SEF) takes place in the proximity of metal structures. The effect of fluorescence enhancement has been intensively studied by several groups¹⁻⁸. In the proximity of metals, the fluorophore radiative properties are modified and an increase in the spontaneous emission rate is observed, which is associated with a concomitant increase in the radiative quantum efficiency. This results from the shortening of the fluorescence lifetime, which enables faster cycling of the fluorophore. These are given by the following relationships:

$$\eta_{ns} = \frac{K_f + K_{ns}}{K_f + K_{ns} + K_i + K_x} \quad (2)$$

$$\tau_{ns} = \frac{1}{K_f + K_{ns}} \quad (3)$$

Here, η_{ns} is the quantum yield, modified by the nanostructure, k_f and k_i are rate constants as in (1), K_{ns} is the additional rate constant induced by the nanostructure and τ_{ns} is the fluorophore lifetime modified by the nanostructures.

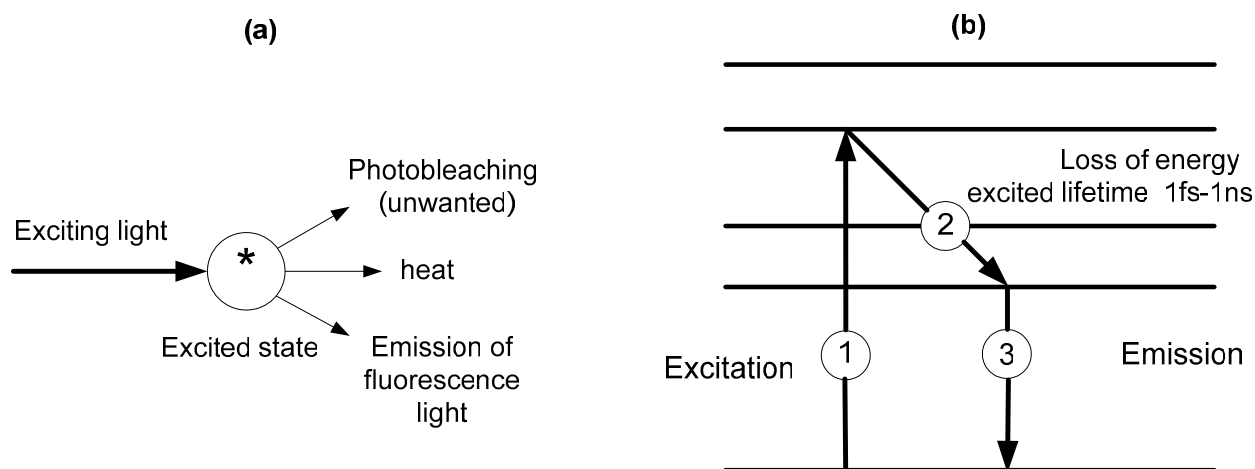


Figure 1: Fluorescence effect: a) molecule is excited by light, b) Schematic explanation of excitation and emission processes, (1) excitation from the ground state, (2) decay to the nearest energy level and (3) photon emission via returning to the ground state.

The fluorophore emission intensity depends on the distance between the metal and the fluorophore in a complex fashion¹⁻³. At very close distances (less than several nm), the fluorophore experiences significant non-radiative decay components, and consequently the emission is strongly quenched. At intermediate distances (e.g. for Ag around 5 nm), the non-radiative decay process subsides and the enhancement effect begins to dominate, producing the overall fluorescence amplification peak, which, for spherical metal nanoparticles, reaches a typical value in the order of 10. For longer distances, (10 nm and above), the amplification tapers off, eventually reaching unity².

Metallic nano-features on different substrates are the most comfortable beds for building optical nano-biosensors in a variety of analytes such as water and blood. They can be formed by conventional nano-lithography techniques on metal substrates or on dielectric substrates, which can be coated with a thin metal film in a following preparation step. A promising option is to prepare the nanostructures with oblique angle deposition techniques (combined with a suitable substrate rotation), thus giving the advantageous possibility to grow nearly arbitrarily shaped, separated nanostructures in a single deposition step without any pre- or post-deposition patterning of the film. The nanostructures deposited with this so-called glancing angle deposition (GLAD) technique can be made of inorganic or organic dielectrics, metals, and

semiconductors, on a variety of substrates⁹. There are 3 reasons that motivated us to investigate such structures for biosensing applications: (i) as metal nanorods they can be used to enhance local electromagnetic fields, (ii) being highly porous, they exhibit large surface to volume ratio and (iii) the possibility of preparing them with different morphologies allows for unique optical properties, such as the polarization-selective reflection from chiral nanostructures.

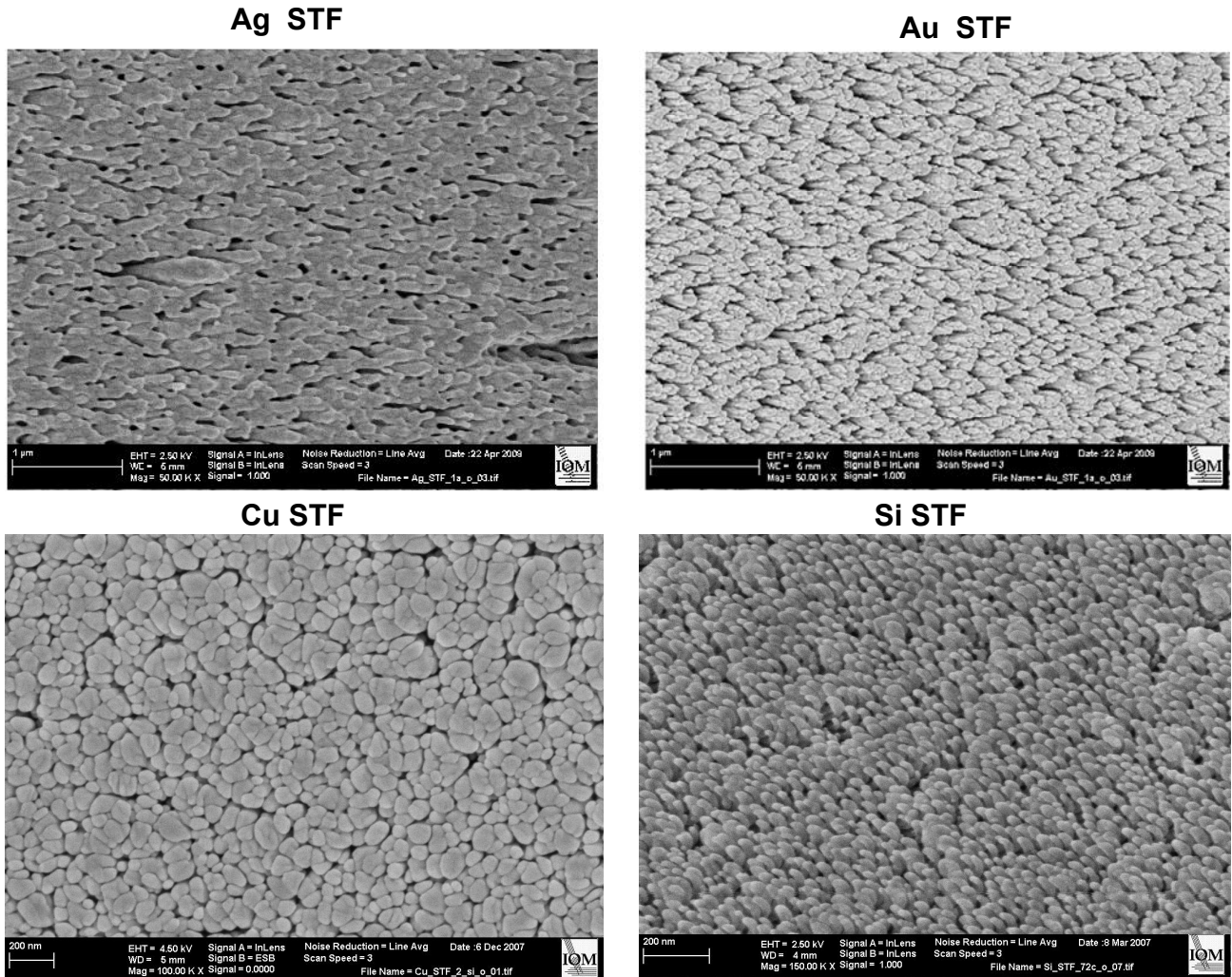


Figure 2: Top-view SEM micrographs of different STF structures prepared for this study.

Sculptured thin films (STFs) are nanostructured materials with unidirectionally varying properties that can be designed and realized in a controllable manner using variants of physical vapor deposition. The ability to virtually instantaneously change the growth direction of their columnar morphology, through simple variations in the direction of the incident vapor flux, leads to a wide spectrum of columnar forms. To date, the chief applications of STFs are in optics as polarization filters, Bragg filters, and spectral hole filters^{10,11}. At visible and infrared wavelengths, a single-section STF is a unidirectionally nonhomogeneous continuum with direction-dependent properties. Several sections can be grown consecutively into a multisection STF, which can be conceived of as an optical circuit that can be integrated with electronic circuitry on a chip. Being porous, an STF can act as a sensor of fluids. Biomedical applications such as tissue scaffolds, drug-delivery platforms, virus traps, and labs-on-a-chip are also in different stages of development. Sculptured thin films (STF) are new potential materials for fluorescent enhancement near the surface. In this work we

investigated the existence of enhanced fluorescence in several STF materials. The origin of the SEF enhancement is questionable as extinction measurements do not show any signs of LSPR excitation in the 400-900nm range.

2. EXPERIMENTAL

The STF samples were prepared using the glancing angle deposition technique. Varieties of samples were prepared using different materials: Si, Ag, Au and Cu on different substrates such as fused silica and Si and with different morphologies such as nanorods and nanohelices. The Si and Cu STF were grown by ion beam sputter GLAD as described elsewhere^{12,13,14} whereas the rodlike Au STFs were grown with DC sputtering and the rodlike Ag STFs by means of electron beam evaporation. The deposition angle was set to approximately 85° in all cases. In figure 2 we present typical scanning electron microscope (SEM) micrographs showing the columnar structure. For reference measurements, continuous film samples of each material were prepared with on-axis deposition. Some of the samples were templated with monolayers of SiO₂ nanospheres using a colloidal self-assembly method¹⁴ and with Au dots in hexagonal arrangements gained by evaporating Au through the holes of such self-assembled films of hexagonally closed packed nanospheres with subsequent removal of the spheres.

For fluorescence measurements, the samples were spin coated with a fluorescent dye Rhodamine 123 diluted in methanol at 0.6%wt. The thickness of the spun dye layer was estimated by atomic force microscope measurements to be approximately 50nm. Care was taken in selecting the spinning conditions to obtain uniform dye films and similar thicknesses both on the sample and its reference. Fluorescence measurements were performed using an Olympus fluorescence microscope with an Hg arc lamp as excitation light source having three fluorescence cubes with the following excitation-emission wavelengths: $\{\lambda_{ex}, \lambda_{em}\} = \{\{365nm, 420nm\}, \{480nm, 505nm\}, \{546nm, 590nm\}\}$. The green Hg line at 546nm was used for excitation in most of the experiments and the emission was detected using the red filter at 590nm. The detection was done using a high sensitivity cooled CCD camera with a controlled exposure time. The grabbed images were then analyzed using Matlab and the average intensity was compared between the sample and its reference. Part of the measurements was also performed using fluorescence spectrometer.

3. RESULTS AND DISCUSSION

Figure 3 shows an example of two fluorescence images, one for a Ag STF (thickness approximately 400 nm) deposited by e-beam evaporation on fused silica. The STF consists of rod-like nanostructures with rod diameter $d \approx 75$ nm, inclined at an angle $\alpha \approx 23^\circ$ with respect to the substrate plane. The left image corresponds to the continuous Ag film used as a reference, which has thickness of approximately 415 nm (deposited on fused silica).

In figure 4 we present fluorescence spectra of different samples with STFs of different elements, grabbed using polarized fluorescence spectrometer where a blue light excitation source (488 nm) was used. As can be seen, the Si spirals on SiO₂ nanospheres shows the least signal comparable to the reference sample, which is a bare Si substrate. The largest enhancement is found for the STF sample containing Cu nanopillars (deposited with fast continuous substrate rotation) on a bare Si substrate.

Table 1 summarizes the main results of this study, showing a wide spectrum of results with the most prominent being the fact that Ag STFs result in the highest fluorescence enhancement factor. The parameters used in the table are defined in figure 5. Ag coated Si STF samples proved to result in a relatively high enhancement factor as well. Cu nanorods on bare Si substrates exhibited the next level of enhancement. According to table 1, Au STFs show no enhancement which is somehow surprising. On the other hand, for the sample containing Si spirals on Au nanodots, an enhancement factor of 4 was observed. It remains unclear whether the Si or the underlying Au dots (dotsize in the range of ≈ 150 nm diameter and approximately 30 nm height) is responsible for this enhancement, thus this might indicate the importance of the size of the Au nanoparticles in determining the fluorescence enhancement. It might also be possible that sometimes the rods in the metal STFs touch each other, thereby forming broader structures, thus canceling the rod lightening effect.

LSPR excitation is not seen from the reflection and transmission spectra that we carried out. Previous works¹⁵ showed that this occurs in the mid-infrared range of the spectrum. The porosity is another factor that can enhance the fluorescence due to larger surface to volume ratio, which we think did not play a role here because the thin film dye used for this study covers mainly the top surface of the sample.

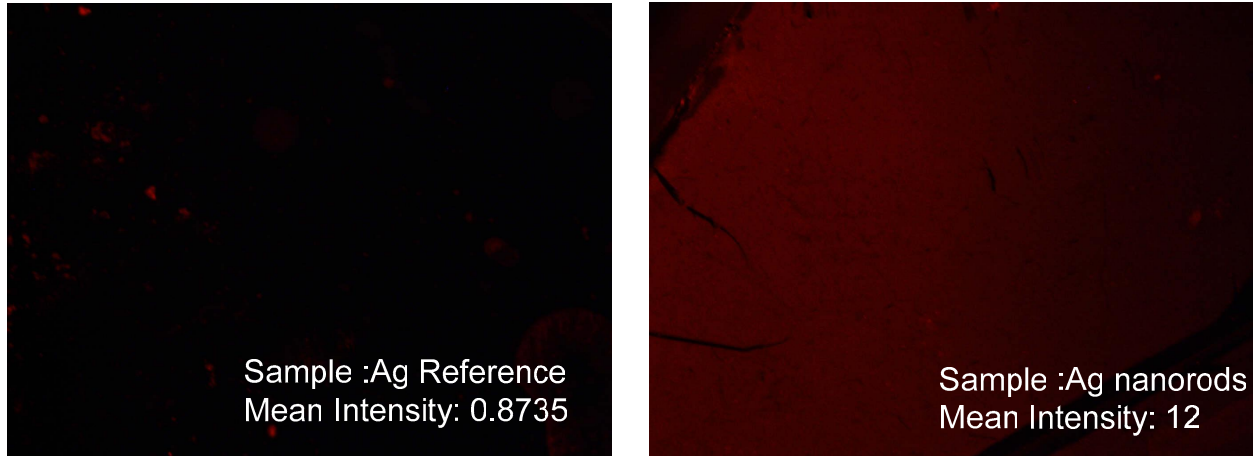


Figure 3: Example of fluorescence images grabbed from closed silver film (left), and columnar silver STF (right), showing an enhancement factor of about 14. The images were originally in red and converted to grey scale.

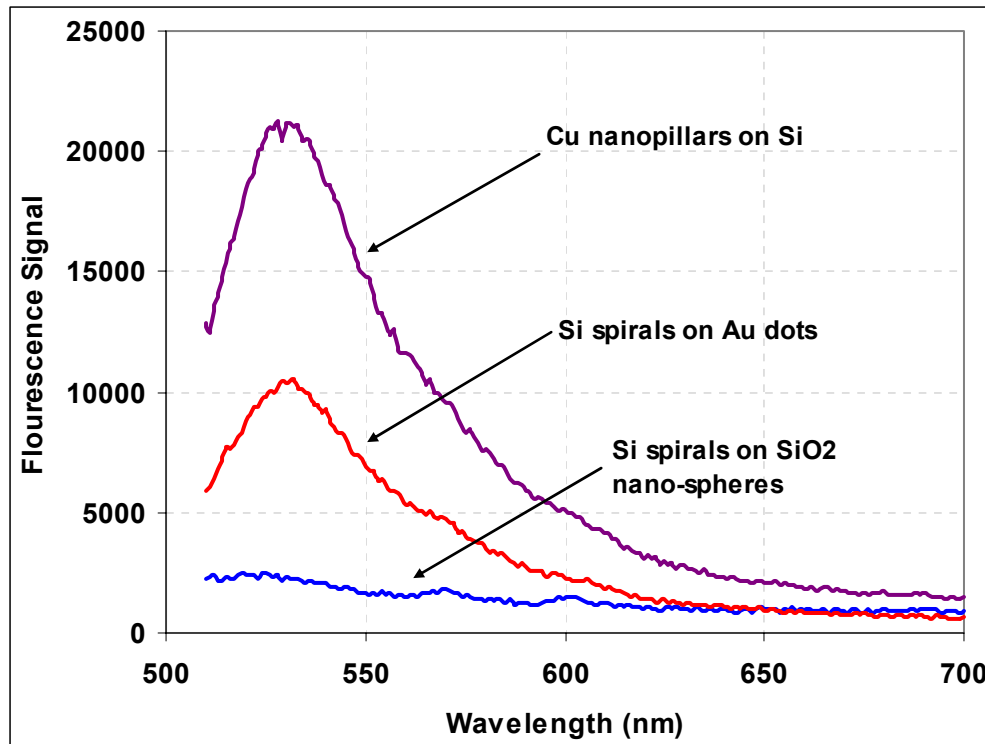


Figure 4: Fluorescence signals versus wavelength from three different samples, showing that the sample consisting of pillar-like Cu structures on bare Si substrates exhibits the largest fluorescence. The fluorophore in this case was excited with 488nm light and the emission is in the green.

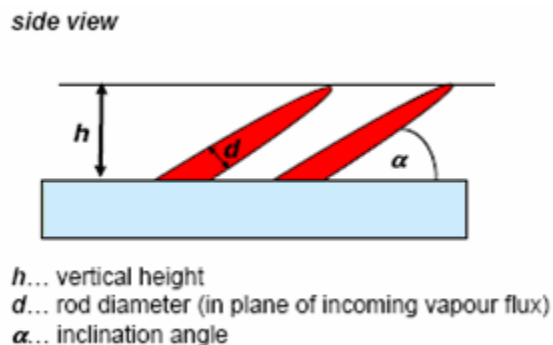


Figure 5: Schematic drawing of rod-like nanostructures grown with GLAD, showing the parameters defining the structure of the STF samples.

Table 1: Summary of the nano-sculptured thin films used in the study and their fluorescence enhancement factors.

Samples	Enhancement factor	Description
Rod - like Ag STF (4 samples)	14	$h=400\text{nm}$, $d=75\text{nm}$, $\alpha=23^\circ$, on fused silica substrate
Si STF with evaporated top layer of Ag on Si (2 samples)	8	Si rods ($h=50\text{nm}$ or 100nm), $\alpha=90^\circ$, on Si substrate and Ag nanolayer (5nm and 15nm) on top
Rod - like Cu STF	8	Cu nanorods 220nm height on Si substrate, $\alpha=90^\circ$
Ag islands (4 samples)	7	5nm and 15nm thick islands of Ag on Si and fused silica substrates
Si STF with evaporated top layer of Ag on fused silica substrate (2 samples)	5	Si rods ($h=50\text{nm}$ or 100nm), $\alpha=90^\circ$, on fused silica substrate and Ag nanolayer (5nm and 15nm) on top
Si spirals on Au nanodots	4	Si spirals, $h=740\text{nm}$, grown on honeycomb like Au nanodots of 30nm height patterned on Si substrate
Si-STF (4 samples)	3	Si rods, $h=50-100\text{nm}$ on Si or glass substrates, $\alpha=90^\circ$
Cu-STF (4 samples)	2	$h=45-100\text{nm}$, $d=30-60\text{nm}$, $\alpha=20^\circ$, on fused silica
Cu-STF (4 samples)	0.5-1	$h=100-1100\text{nm}$, $d=40-150\text{nm}$, $\alpha=30-42^\circ$, on fused silica substrate
Si spirals on SiO_2 nanospheres	0.5-1	$h = 1090\text{nm}$, Si substrate templated with monolayer of SiO_2 nanospheres (diameter 350 nm)
Rod - like Au STF	0.5-1	$h=285\text{nm}$, $d=40\text{nm}$, $\alpha=35^\circ$, on fused silica substrate

4. CONCLUSIONS

To conclude, fluorescence enhancement was observed on metallic sculptured thin films mostly prominent in films containing Ag nanorods, Ag islands or thin (<20 nm) coating of GLAD-grown Si nanorods with an Ag top layer. The enhancement factor is found to be as high as 14. Upright, pillar-like nanostructures of Cu on bare Si substrates also exhibited fluorescence enhancement up to a factor of 8. Si spirals on top of Au nanodots exhibited some noticeable enhancement by a factor of 4. Au and Cu STF samples with inclination angle to the substrates in the range $20^\circ-42^\circ$ exhibited no enhancement possibly due to touching of the rods, thus cancelling out the lightning rod effect. LSPR excitation was not observed in the spectral range of 400-1100 nm. The porosity is believed not to play a role here

because the thin film dye used covers mainly the top surface of the sample. This study shows the potential of metal based STFs as suitable beds for fluorescence based sensing. Further studies are going on for the possibility of bacteria sensing in water using the enhanced fluorescence observed in Ag based samples.

Acknowledgement:

This work is supported by the Israel Ministry of Sciences under the “Tashtiot” program and by the DFG within project P3 of the research group 522 “Architecture of nano- and microdimensional structure elements”.

REFERENCES

- [1] J.R. Lakowicz, Y. Shen, S. D’Auria, J. Malicka, J. Fang, Z. Gryczynski, I. Gryczynski, “Radiative Decay Engineering 2. Effects of Silver Island Films on Fluorescence Intensity, Lifetimes, and Resonance Energy Transfer,” *Anal. Biochem.* 301, 261-277 (2002).
- [2] E.M. Goldys, A. Barnett, F. Xie, K. Drozdowicz-Tomsia, I. Gryczynski, E.G. Matveeva, Z. Gryczynski, T. Shtoyko, “Plasmon-enhanced fluorescence near metallic nanostructures: biochemical applications,” *Appl. Phys. A* 89, 265–271 (2007).
- [3] Yongxia Zhang, Kadir Aslan, Michael J. R. Previte, Chris D. Geddes, “Metal-enhanced fluorescence from copper substrates,” *Appl. Phys. Lett.* 90, 173116-18 (2007).
- [4] Jian Zhang, Joanna Malicka, Ignacy Gryczynski, and Joseph R. Lakowicz, “Surface-Enhanced Fluorescence of Fluorescein-Labeled Oligonucleotides Capped on Silver Nanoparticles,” *J. Phys. Chem. B*, 109, 7643 -7648 (2005).
- [5] Fang Xie, Mark S. Baker and Ewa M. Goldys, “Homogeneous Silver-Coated Nanoparticle Substrates for Enhanced Fluorescence Detection,” *J. Phys. Chem. B*, 110 (46), 23085 -23091 (2006).
- [6] Evgenia Matveeva, Zygmunt Gryczynski, Joanna Malicka, Ignacy Gryczynski and Joseph R. Lakowicz, “Metal-enhanced fluorescence immunoassays using total internal reflection and silver island-coated surfaces, *Analytical Biochemistry*,” 334, 303-311 (2004).
- [7] Jung-Hoon Song, Tolga Atay, Sufei Shi, Hayato Urabe, and Arto V. Nurmikko, “Large Enhancement of Fluorescence Efficiency from CdSe/ZnS Quantum Dots Induced by Resonant Coupling to Spatially Controlled Surface Plasmons,” *Nano Lett.*, 5 (8), 1557 -1561 (2005).
- [8] Felicia Tam, Glenn P. Goodrich, Bruce R. Johnson, and Naomi J. Halas, “Plasmonic Enhancement of Molecular Fluorescence,” *Nano Lett.*, 7 (2), 496 -501, 2007.
- [9] A. Lakhtakia and R. Messier, [Sculptured Thin Films: Nanoengineered Morphology and Optics], SPIE Press, Bellingham, WA, USA, (2005).
- [10] I. J. Hodgkinson, Q. H. Wu, K. E. Thorn, A. Lakhtakia, and M. W. McCall, “Spacerless circular-polarization spectral-hole filters using chiral sculptured thin films: theory and experiment,” *Opt. Commun.* 184, 57-66 (2000).
- [11] A. C. van Popta, M. M. Hawkeye, J. C. Sit, and M. J. Brett, “Gradient-index narrow-bandpass filter fabricated with glancing-angle deposition,” *Opt. Lett.* 29, 2545 (2004).
- [12] E. Schubert, T. Höche, F. Frost, B. Rauschenbach, “Nanostructure fabrication by glancing angle ion beam assisted deposition of silicon,” *Appl. Phys. A* 81, 481-486 (2005).
- [13] Ch. Patzig, B. Rauschenbach, W. Erfurth, A. Milenin, “Ordered silicon nanostructures by ion beam induced glancing angle deposition,” *J. Vac. Sci. Technol. B* 35, 833-838 (2007).
- [14] B. Fuhrmann, H.S. Leipner, H.R. Höche, L. Scubert, P. Werner, U. Gösele, “Ordered Arrays of Silicon Nanowires Produced by Nanosphere Lithography and Molecular Beam Epitaxy,” *Nano Lett.* 5, 2524-27 (2005).
- [15] A. I. Maarouf, A. Gentle, G. B. Smith and M. B. Cortie, “Bulk and surface plasmons in highly nanoporous gold films,” *J. Phys. D: Appl. Phys.* 40, 5675-82 (2007).